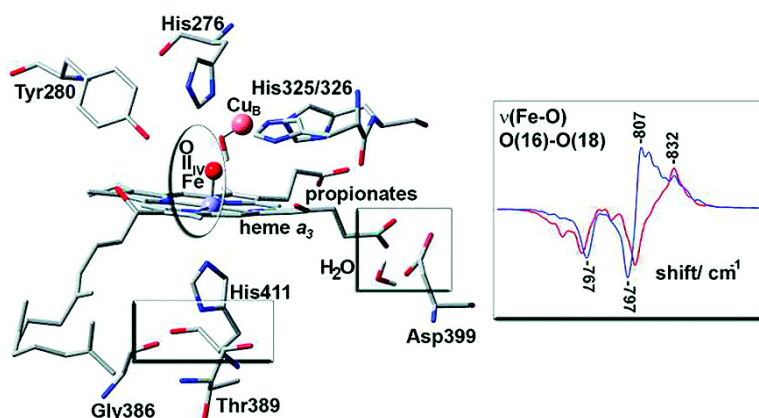Article

Assigning Vibrational Spectra of Ferryl-Oxo Intermediates of Cytochrome *c* Oxidase by Periodic Orbits and Molecular Dynamics

Vangelis Daskalakis, Stavros C. Farantos, and Constantinos Varotsis

More About This Article

Additional resources and features associated with this article are available within the HTML version:

- Supporting Information
- Access to high resolution figures
- Links to articles and content related to this article
- Copyright permission to reproduce figures and/or text from this article

View the Full Text HTML

Assigning Vibrational Spectra of Ferryl-Oxo Intermediates of Cytochrome *c* Oxidase by Periodic Orbits and Molecular Dynamics

Vangelis Daskalakis,[†] Stavros C. Farantos,*,[†,‡] and Constantinos Varotsis[‡]

Institute of Electronic Structure and Laser, Foundation for Research and Technology-Hellas (FORTH), P.O. Box 1527, 71110, Voutes-Heraklion, Crete, Greece, and Department of Chemistry, University of Crete, P.O. Box 2208, 71305, Voutes-Heraklion, Crete, Greece

Received March 12, 2008; E-mail: farantos@iesl.forth.gr

Abstract: Complexity is inherent in biological molecules not only because of the large number of atoms but also because of their nonlinear interactions responsible for chaotic behaviours, localized motions, and bifurcation phenomena. Thus, versatile spectroscopic techniques have been invented to achieve temporal and spacial resolution to minimize the uncertainties in assigning the spectra of complex molecules. Can we associate spectral lines to specific chemical bonds or species in a large molecule? Can energy stay localized in a bond for a substantial period of time to leave its spectroscopic signature? These longstanding problems are investigated by studying the resonance Raman spectra of ferryl-oxo intermediates of cytochrome *c* oxidase. The difference spectra of isotopically substituted ferryl oxygen (^{16}O minus ^{18}O) in the cytochrome *c* oxidase recorded in several laboratories show one or two prominent positive peaks which have not been completely elucidated yet. By applying the hierarchical methods of nonlinear mechanics, and particularly the study of periodic orbits in the active site of the enzyme, in conjunction with molecular dynamics calculations of larger systems which include the embraced active site by the protein and selected protonated/deprotonated conformations of amino acids, we translate the spectral lines to molecular motions. It is demonstrated that for the active site stable periodic orbits exist for a substantial energy range. Families of periodic orbits which are associated with the vibrations of $Fe^{IV}=O$ bond mark the regions of phase space where nearby trajectories remain localized, as well as assign the spectral bands of the active site in the protein matrix. We demonstrate that proton movement adjacent to active site, which occurs during the P → F transition, can lead to significant perturbations of the $Fe^{IV}=O$ isotopic difference vibrational spectra in cytochrome *c* oxidase, without a change in oxidation state of the metal sites. This finding links spectroscopic characteristics to protonation events occurring during enzymatic turnover.

I. Introduction

Polyatomic molecules are complex systems with nonlinear interactions and that makes the study of dynamical processes difficult. For example, a simple isomerization reaction which takes place in an active site of a protein will involve the break and the formation of chemical bonds after the excitation of the site at energies above potential barriers. In such cases, the appearance of nonlinear phenomena, like resonances and chaos,[1] are inevitable and such phenomena have been observed spectroscopically.[2] Selectivity and specificity are well-established concepts in elementary chemical reactions when the role of mode excitation in the reactant molecules and the energy disposal in the products are investigated. Triatomic molecules have been used as prototypes to develop theories as well as to build sophisticated experimental apparatus in order to study elementary chemical reactions at the molecular level and at the femtosecond time scales.[3] The small number of degrees of freedom in these systems has allowed a detailed analysis of the correspondence between quantum and classical theories.[4]

Nonlinear mechanics offer a systematic method to study complex systems. The hierarchical detailed exploration of the molecular phase space requires first the location of the equilibrium points of the potential function and then the location of periodic orbits (POs), the tori around stable POs, stable and unstable manifolds for the unstable POs, and even transition state objects such as the normally hyperbolic invariant manifolds.[5] Such a program has been implemented up to now to two and three degrees of freedom models for triatomic molecules.[6−9] This work has revealed the importance of periodic

[†] Foundation for Research and Technology-Hellas (FORTH).
[‡] University of Crete.

(1) Wiggins, S. *Introduction to Applied Nonlinear Dynamical Systems and Chaos*, 2nd ed.; Springer-Verlag: New York, 2003.
(2) Ishikawa, H.; Field, R. W.; Farantos, S. C.; Joyeux, M.; Koput, J.; Beck, C.; Schinke, R. *Annu. Rev. Phys. Chem.* **1999**, *50*, 443–484.
(3) Zewail, A. H. *J. Phys. Chem. A* **2000**, *104*, 5660–5694.
(4) Joyeux, M.; Grebenshchikov, S.; Yu. Bredenbeck, J.; Schinke, R.; Farantos, S. C. *Adv. Chem. Phys.* **2005**, *130*, 267–303.
(5) Uzer, T.; Jaffé, C.; Palacián, J.; Yanguas, P.; Wiggins, S. *Non-linearity* **2002**, *15*, 957–992.
(6) Main, J.; Jung, C.; Taylor, H. S. *J. Chem. Phys.* **1997**, *107*, 6577–6583.
(7) Svitak, J.; Li, Z.; Rose, J.; Kellman, M. E. *J. Chem. Phys.* **1995**, *102*, 4340–4354.
(8) Joyeux, M.; Farantos, S. C.; Schinke, R. *J. Phys. Chem.* **2002**, *106*, 5407–5421.
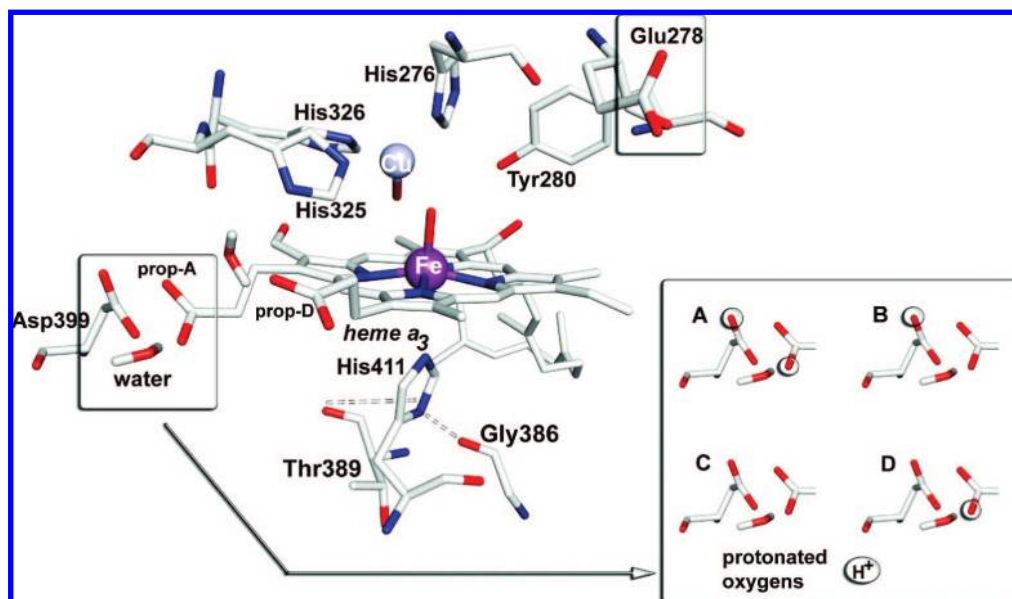
Figure 1. Crystal structure of the aa_3 cytochrome c oxidase from *Paracoccus denitrificans*. Heme a_3–Fe/Cu$_B$ active site is shown. In the proximal area, amino acids Gly386 and Thr389 are in close proximity to the His411 which coordinates to heme a_3–Fe. (Inset) Different protonated/deprotonated states of the A-propionate–Asp399 pair. In structures A and C, all carboxyl groups in equilibrium are protonated or deprotonated, respectively, while in B or D structures only one H$^+$ is available protonating either Asp399 or propionate, respectively. Carbon appears gray, oxygen red, and nitrogen blue, and white is used for hydrogen.

orbits in elucidating nonlinear effects in vibrational spectroscopy and the good correspondence between classical and quantum mechanics particularly for overtone states.

In studying large molecules such as biological ones, the application of systematic methods of nonlinear mechanics becomes a challenge, since not only more computer power is needed but also the development of concepts and techniques to extract the physics from the calculations. It is not surprising that up to now statistical mechanical methods have mainly been used, implemented by either averaging over phase space points or over transition paths.[10] On the other hand, the systematic approach to explore polyatomic molecules is usually exhausted by the location of equilibrium points (minima and saddles), to be followed with the calculation of phase space.[11] Methods to incorporate quantum effects in reaction dynamics have been proposed.[12]

Efforts to find localized motions in infinite periodic or random anharmonic lattices have led to the concept of discrete breathers.[13,14] The initial observations of localized motions in the work of Sievers and Takeno[15] brought a lot of surprise to physicists and triggered the discovery of significant mathematical theorems for the existence of periodic orbits in infinite dimensional lattices.[13] Biomolecules, although not periodic, have given evidence for localized motions.[16]

Vibrational localization is a familiar concept to chemists, and very early they noticed that transition from normal mode vibrations to local modes involve an elementary bifurcation in classical mechanics.[17] Biochemists frequently associate biochemical action to specific sites in a protein. Such a case is cytochrome c oxidase (CcO), the terminal enzyme in the respiratory chains, found in the inner mitochondrial membranes or in many bacteria, and it is the last acceptor of electrons from oxidizing processes involving nutrient molecules. CcO facilitates the activation and four-electron reduction of oxygen molecule to water with the pump of four protons across the inner mitochondrial membrane attributing to the electrochemical gradient[18] that is used to drive the synthesis of ATP. CcO is particularly appealing for theoretical studies, because of the relative small size of its active site as well as there is a plethora of experimental results in the literature. Nevertheless, details of its molecular mechanism of action are still unclear, being a matter of considerable debate for over two decades. A recent review article on the role of CcO in proton translocation, as well as intermediate compounds and reaction mechanisms are given in ref 19.

Electrons from cytochrome c pass through a bimetallic Cu$_A$–Cu$_A$ site to the binuclear high-spin heme a_3/Cu$_B$ active site via a low-spin heme a. Figure 1 depicts the active site from aa_3 enzyme of *Paracoccus denitrificans* (protein data bank (PDB) code 1AR1).[20] aa_3 cytochrome c oxidases have extensively been studied on reaction with molecular O$_2$. Because of its smaller size, we have constructed a model of *Paracoccus denitrificans* CcO, whose subunits I, II, and III show a high degree of homology with those of beef heart CcO (PDB code 1OCC). A covalent bond was added between His276 N$_{\epsilon 2}$ and Tyr280 C$_{\epsilon 2}$.

(9) Jung, C.; Taylor, H. S. *J. Phys. Chem. A* **2007**, *111*, 3047–3068.

(10) Dellago, Ch; Bolhuis, P. G.; Geissler, P. L. *Adv. Chem. Phys.* **2002**, *123*, 1–78.

(11) Wales, D. *Energy Landscapes with Applications to Clusters, Biomolecules and Glasses*; Cambridge University Press: London, 2003.

(12) Truhlar, D. G.; Gao, J.; Alhambra, C.; Garcia-Viloca, M.; Corchado, J.; Sánchez, M. L.; Villá, J. *Acc. Chem. Res.* **2002**, *35*, 341–349.

(13) Aubry, S. *Physica D* **1997**, *103*, 201–250.

(14) Campbell, D. K.; Flach, S.; Kivshar, Y. S. *Phys. Today* **2004**, *57*, 43–49.

(15) Sievers, A. J.; Takeno, S. *Phys. Rev. Lett.* **1988**, *61*, 970–973.

(16) Xie, A.; van der Meer, L.; Hoff, W.; Austin, R. H. *Phys. Rev. Lett.* **2000**, *84*, 5435–5438.

(17) Lawton, R. T.; Child, M. S. *Mol. Phys.* **1981**, *44*, 709–723.

(18) Wikström, M. K. *Nature* **1977**, *266*, 271–273.

(19) Belevich, I.; Verkhosky, M. I. *Antioxid. Redox Signaling* **2008**, *10*, 1–29.

(20) Ostermeier, C.; Harrenga, A.; Ermler, U.; Mechel, H. *Proc. Natl. Acad. Sci. U.S.A.* **1997**, *94*, 10547–10553.

In Figure 1 we can see that the fifth axial ligand of heme a_3 iron is a histidine residue, called proximal histidine (His411), whereas Cu_B coordinates to three histidine residues (His276, His325, and His326, according to the aa_3 *Paracoccus denitrificans* numbering). The experimentally detected iron a_3 redox states are Fe^{II}, Fe^{III}, and Fe^{IV}, while for the copper metal they are Cu_B^I and Cu_B^{II}. Molecular oxygen binds to heme a_3 iron forming the first intermediate. Reduction by three electrons induces O–O bond cleavage producing species with ferryl-oxo (heme a_3–Fe^{IV}=O) character,[21] whereas a hydroxyl ligand coordinates Cu_B^{II} (see ref 19 for details). In the reaction of the mammalian mixed valence form of CcO with O_2, in which only heme a_3 and Cu_B are reduced, the P_M intermediate (607 nm species) exhibits a band with prominent frequency, ω, at 804 cm^{-1} probed by resonance Raman (RR) spectroscopy, which has been attributed to the Fe=O bond.[22] In contrast to that, in the reaction of the fully reduced enzyme with O_2, either two bands are identified in the difference spectra exhibiting ferryl-oxo character (P_R) with prominent frequencies at 790 and 804 cm^{-1} or only the former.[23–25] The two peaks are shifted by 40 cm^{-1} to 750 and 764 cm^{-1}, respectively, with $^{18}O_2$ isotopic substitution. Can we indeed assign these peaks to the ferryl-oxo bond or to collective motions of the active site? What causes the appearance of one or two bands observed in different laboratories?

Recently, Cascella and co-workers[26] have shown the crucial effects of the protein frame for the electronic and structural properties of the copper active site in azurin. In our case, the environment of the heme a_3 could be altered by the formation of the water or the pumping of protons. The importance of these particular interactions has been identified in ba_3 from *Thermus thermophilus*. It has been suggested that the so-called water pool is part of the proton exit channel, and the primary acceptor for both pumped protons and H_2O molecules that are formed at the binuclear center of the enzyme.[27–29] Moreover, there is some evidence in the ba_3 oxidase for an equilibrium between propionate-Asp372 and a water molecule.[29] Therefore, it is essential to elucidate the protein dynamics near the H_2O–Asp372–heme a_3–Cu_B site, which includes one of the strongest interactions between different groups in heme–copper oxidases (propionate A and Asp372 carboxyl groups are only 3.3 Å apart).[30] The accumulation of H_2O molecules has been identified

in the *P. denitrificans* oxidase and its involvement in proton exit channels has been demonstrated by mutagenesis experiments.[30,31]

Proton pathways are important for the function of the terminal oxidases like CcO. Proton movement involves protonation of water molecules or protonation/deprotonation of amino acids resulting in local changes of the electrostatic potential.[19] Some evidence has been given in the study of ba_3 oxidase and the so-called Q-channel.[27–29,32] For example, different protonation states of the A-propionate as well as for the Asp399 residue (aa_3 *P. denitrificans* numbering) are presented in the inset of Figure 1 according to the previous studies of ba_3[29] and the important functional role of Asp399 in proton translocation in aa_3 from *P. denitrificans*.[33] In addition, Glu278 residue in the entrance of the so-called D-proton pathway[19] has been proposed to play a possible role as a proton shuttle[34] or a switch based on its protonation state coupled to the ability of a proton to propagate along this path[35] or to local structural changes in the region of propionates.[36–38]

What is the impact of these protonated/deprotonated amino acids to the spectra of ferryl-oxo intermediates?

In this article, we apply a systematic method to interpret the peaks that appear in the difference RR spectra of isotopically substituted ferryl oxygen (^{16}O minus ^{18}O). First, a detailed study of the active site is carried out. Density functional theory calculations are employed to find equilibrium structures, harmonic frequencies and charge distributions for the active site. These data together with the force fields Amber99[39] and CHARMM27[40] are used to construct a realistic potential function for the active site as well as the total enzyme. Then, periodic orbits that emanate from the equilibrium point of the active site are located for several energies. We may consider these periodic orbits as the nonlinear mechanical counterparts of the normal modes that semiclassically correspond to quantum overtone states. Thus, conclusions for the realistic anharmonic potential and the excited vibrational states can be extracted. In the second part of this work, we calculate vibrational frequencies by molecular dynamics associated with the $Fe^{16}O$ and $Fe^{18}O$ bonds for different protonation states of important carboxyl groups in the protein matrix. In this way, we are able to compare calculated difference spectra to experimental ones, and we investigate how the protein environment affects the motion of ferryl-oxo species, and thus its spectrum.

(21) Varotsis, C.; Zhang, Y.; Appelman, E. H.; Babcock, G. T. *Proc. Natl. Acad. Sci. U.S.A.* **1993**, *90*, 237–241.

(22) Proshlyakov, D. A.; Pressler, M. A.; Babcock, G. T. *Proc. Natl. Acad. Sci. U.S.A.* **1998**, *95*, 8020–8025.

(23) Varotsis, C.; Babcock, G. T. *Biochemistry* **1990**, *29*, 7357–7362.

(24) Ogura, T.; Hirota, S.; Proshlyakov, D. A.; Shinzawa-Itoh, K.; Yoshikawa, S.; Kitagawa, T. *J. Am. Chem. Soc.* **1996**, *118*, 5443–5449.

(25) Han, S.; Takahashi, S.; Rousseau, D. L. *J. Biol. Chem.* **2000**, *275*, 1910–1919.

(26) Cascella, M.; Magistrato, A.; Tavernelli, I.; Carloni, P.; Rothlisberger, U. *Proc. Natl. Acad. Sci. U.S.A.* **2006**, *103*, 19641–19646.

(27) Soulimane, T.; Buse, G.; Bourenkov, G. P.; Bartunik, H. D.; Huber, R.; Than, M. E. *EMBO J.* **2000**, *19*, 1766–1776.

(28) Than, M. E.; Soulimane, T. ba3 Cytochrome c Oxidase from Thermus thermophilus. In *Handbook of Metalloproteins*; Messerschimdt, A., Huber, R., Poulos, T., Wieghardt, K., Eds.; John Wiley and Sons, Ltd.: Chichester, UK, 2001; pp 363–378.

(29) Koutsoupakis, K.; Soulimane, T.; Varotsis, C. *Biophys. J.* **2004**, *86*, 2438–2444.

(30) Kannt, A.; Lancaster, C. R. D.; Michel, H. *Biophys. J.* **1998**, *74*, 708–721.

(31) Ostermeier, C.; Iwata, S.; Michel, H. *Curr. Opin. Struct. Biol.* **1996**, *6*, 460–466.

(32) Ohta, T.; Pinakoulaki, E.; Soulimane, T.; Kitagawa, T.; Varotsis, C. *J. Phys. Chem. B* **2004**, *108*, 5489–5491.

(33) Pfitzner, U.; Hoffmeier, K.; Harrenga, A.; Kannt, A.; Michel, H.; Bamberg, E.; Richter, O-M. H.; Ludwig, B. *Biochemistry* **2000**, *39*, 6756–6762.

(34) Kaila, V. R. I.; Verkhovsky, M. I.; Hummer, G.; Wikström, M. K. *Proc. Natl. Acad. Sci. U.S.A.* **2008**, *105*, 6255–6259.

(35) Xu, J.; Voth, G. A. *Proc. Natl. Acad. Sci. U.S.A.* **2005**, *102*, 6795–6800.

(36) Svensson-Ek, M.; Abramson, J.; Larsson, G.; Tornröth, S.; Brzezinski, P.; Iwata, S. *J. Mol. Biol.* **2002**, *321*, 329–339.

(37) Wikström, M. K.; Ribacka, C.; Molin, M.; Laakkonen, L.; Verkhovsky, M.; Puustinen, A. *Proc. Natl. Acad. Sci. U.S.A.* **2005**, *102*, 10478–10481.

(38) Seibold, S. A.; Mills, D. A.; Ferguson-Miller, S.; Cukier, R. I. *Biochemistry* **2005**, *44*, 10475–10485.

(39) Wang, J.; Cieplak, P.; Kollman, P. A. *J. Comput. Chem.* **2000**, *21*, 1049–1074.

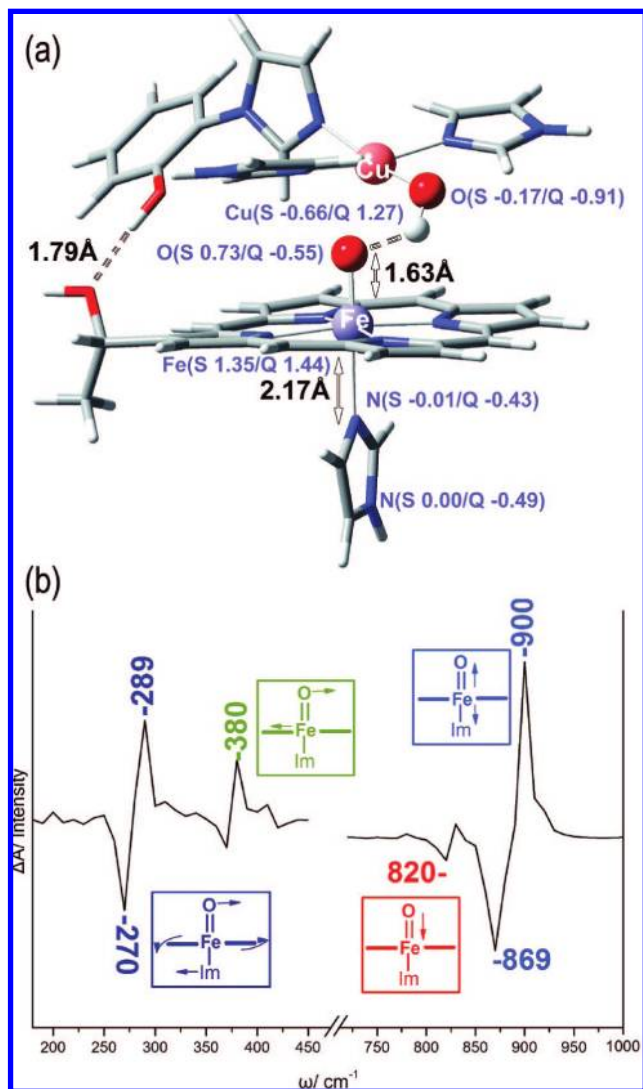(40) Foloppe, N.; MacKerell, A. D., Jr *J. Comput. Chem.* **2000**, *21*, 86–104.

Figure 2. (a) Fully optimized in geometry structure of the active site with ferryl-oxo (^{16}O) character in the b3lyp/6-311g* level of theory. Selected interatomic distances (like imidazole–Fe and Fe–O) are shown in black. Mulliken calculated spin (S) and charge (Q) populations are also shown (blue) for the atoms Fe, NA/NB (imidazole), ferryl oxygen, Cu_B, and oxygen on Cu_B. (b) Calculated vibrational difference spectrum (^{16}O minus ^{18}O) at the b3lyp/6-311g* level of theory, exhibiting features of Fe–O stretching (750–950 cm^{-1} region) and bending (250–400 cm^{-1} region) for the optimized structure of model in (a). Graphical representation of selected modes corresponding to peaks in the spectrum are shown.

II. Computational Methods

We have designed one model molecule of the active site of cytochrome *c* oxidase (Figure 2a). The model contains (a) a Cu^{II} metal coordinated to two imidazoles, a cross-linked imidazole–phenol unit and a hydroxyl (–OH) group and (b) a heme–Fe^{IV} center, in which the axial coordination of ferryl iron contains an imidazole and an oxo (O^{2-}) ligand. The heme a_3 is taken without the propionate groups (see Figure 1), and it is represented by an iron porphyrin with only a CH(OH)CH$_3$ group substituting the hydroxy-ethylfarnesyl side chain. This latter group interacts via a hydrogen bond with the cross-linked protonated phenol. The model is justified by the work of Pinakoulaki et al.[41] in which oxygenated intermediates are formed with similar spectroscopic characteristics by mixing oxygen with the CO-bound mixed valence wild type and Y280H aa_3 enzymes from *P. denitrificans*.

(41) Pinakoulaki, E.; Pfitzner, U.; Ludwig, B.; Varotsis, C. *J. Biol. Chem.* **2002**, *277*, 13563–13568.

A full geometry optimization (unrestricted open-shell) was performed by using the hybrid density functional b3lyp method. We used the 6-311g(d) triple-ζ basis set as implemented in the Gaussian03 software package.[42] The choice of method and basis set is justified by previous studies on the active site of such enzymes, producing correct energies and geometries even at lower levels of theory (b3lyp/6-31g*),[43] as compared to experimental data.

Subsequently, evaluation of the Hessian matrix of optimized model and a highly expensive computation of the harmonic vibrational spectrum took place. No restrictions were applied on the geometries during optimization. The Mulliken method[44] was also employed in the same software package to calculate spin populations and charges on all atoms (see Figure 2a). The calculated spin populations are consistent with a ferryl Fe^{IV}=O character, as previously described in theory by Blomberg's group.[43] In addition to the ^{16}O model, harmonic vibrational frequencies of the isotopic substituted ferryl oxo ligand ($^{18}O^{2-}$) and hydroxyl oxygen (–^{18}OH) on Cu have been obtained.

The periodic orbit analysis has been described extensively in previous publications.[45] To find periodic orbits, i.e., to close a trajectory in phase space, is equivalent to solve a two point boundary value problem. We achieve that iteratively with shooting techniques and integrating Hamilton's equations of motion. The stability of periodic orbits is determined by calculating the eigenvalues of the monodromy matrix and the continuation of a family of periodic orbits is done by a linear extrapolation in the period of periodic orbit. Stable POs mean that the region of phase space around the periodic orbits is occupied by quasiperiodic trajectories (tori), whereas unstable periodic orbits imply the existence of degrees of freedom from where nearby trajectories can escape to remote regions of phase space. The calculations were performed with the program POMULT[46] in conjunction with TINKER[47] suite of programs which provides the potential and its first and second derivatives. The POs were closed in coordinates and momenta with accuracy at least 1×10^{-4}. The units used are consistent with distances in angstroms, energy in kcal/mol, and time in picoseconds.

Molecular dynamics simulations were carried out with initial Cartesian coordinates from the two-subunit aa_3 crystal structure of *Paracoccus denitrificans* (PDB code 1AR1). Only one chain (including parts of subunits I and II) is used in our simulations with around 9000 atoms in the A, B, C, and D protonation cases of propionate–Asp399 pair[29] discussed above (Figure 1) and protonated/deprotonated Glu278. Partial charges for Mg/Ca/Cu$_A$–Cu$_A$/heme a/heme a_3/Cu$_B$ metal sites were derived from DFT optimized models (b3lyp/6-311g* level). All crystallographic water molecules were retained in the structure (TIP3P force field). Simulations were performed at constant energy, which corresponds to an average temperature of 300 K. For the integration of equations of motion, a time step of 0.15 fs was used. The software package Tinker 4.2[47] was employed with the Amber99[39] force field. Several parameters, especially for the heme groups, were fitted to DFT data or taken from CHARMM27[40] force field and altered accordingly to fit our DFT or the experimental data. The bond type parameter was set to Morse. All amino acids were free to move during the simulations, except one case where a force constant of 7 kcal/mol Å was applied to restrain the distance between the C$_\gamma$

(42) Frisch, M. J.; Trucks, G. W.; Schlegel, H. B.; Scuseria, G. E.; Robb, M. A.; Cheeseman, J. R.; Montgomery, J. A., Jr.; Vreven, T.; Kudin, K. N.; Burant, J. C.; et al. *Gaussian03, Revision B.03*; Gaussian: Wallingford, CT, 2004.
(43) Blomberg, R. A. M.; Siegbahn, E. M. P. *Inorg. Chem.* **2003**, *42*, 5231–5243.
(44) Mulliken, R. S. *J. Chem. Phys.* **1955**, *23*, 1833–1840, ibid. 1841–1846, 2338–2342, 2343–2346.
(45) Farantos, S. C. *Comput. Phys. Commun.* **1998**, *108*, 240–258.
(46) Farantos, S. C. *J. Chem. Phys.* **2007**, *126*, 175101–175107.
(47) Ponder J. W. 2004 *TINKER-Software tools for molecular design, Version 4.2*; Department of Biochemistry and Molecular Biophysics, Washington University School of Medicine: St. Louis, MO, September 2004.

atom of Glu278 and the Δ-methyl carbon of heme a_3 at its crystallographic value as proposed elsewhere.[37] For nonbonded interactions a cutoff distance of 12 Å with a smoothing window between 9.6 and 12 Å was applied. Structures were minimized and equilibrated before each simulation.

Time-bond distance series are recorded for every molecular dynamics simulation. Two different methods are used to derive the vibrational power spectra (Raman transition moments are not taken into account): (a) fast fourier Transform (FFT) over time−distance series from one trajectory (1.2 ns), using one CPU and (b) averages of FFTs of around 100 50-ps trajectories, using 500 CPUs on EGEE (Enabling Grids for E-SciencE) Grid. Throughout each 1.2 ns simulation (protonation cases A, B, C, D with Glu278 protonated or deprotonated), structures obtained every 10 ps were used as initial conditions for the 100 50-ps trajectories run. In the following, we present the results of the 1.2 ns simulations. The integration time is considered to be adequate for convergence, since after 0.6 ns positions and intensities of the peaks in the spectra remain unchanged.

III. Results and Discussion

A. Density Functional Theory Calculations. The difference spectrum (^{16}O minus ^{18}O) for the model active site is shown in Figure 2b at the b3lyp/6-311g* level of theory. Common DFT methods overestimate the force constants. When vibrational frequencies are calculated by electronic structure theory, they can often be improved by scaling, and it is useful to have general scaling factors. Such factors depend on the level of electronic structure theory and the one-electron basis set, as well as on the specific system, and they are expected to lower the calculated Fe−O stretching by anharmonic corrections.[48,49] In our case, we do not multiply with such a common factor, but instead, we present the original calculated frequencies. However, we scale the force constants in the fitted potential to reproduce the experimental frequencies of Fe−O stretch.

In Figure 2b we distinguish two frequency ranges: the 750−950 cm^{-1}, which corresponds to the Fe−O stretching modes, and 270−380 cm^{-1}. The latter is attributed to the bending vibrations of the O=Fe−imidazole moiety of the model. Such vibrations have been proposed to appear experimentally at 250−400 cm^{-1} range by Kitagawa's,[24] Rousseau's,[25] Babcock's,[22,21] Varotsis',[50] and Ogura's[51] research groups. The purpose of this article is to analyze the stretch vibrations, since this range of frequencies is the most studied in cytochrome *c* oxidases by infrared and Raman spectroscopy.

B. Periodic Orbits and Molecular Dynamics of the Active Site. The density functional theory provided data to construct a reliable potential energy surface for the active site of C*c*O. The resulting anharmonic analytical potential employs Morse type functions for the stretches, harmonic potentials for the angles, cosine functions for the torsions, and Lennard-Jones and Coulomb intermolecular interactions.[52] The set of fitted parameters reasonably reproduces the data.

The harmonic vibrational normal modes are valid only for very small deviations from the minimum of the potential. Anharmonicity and couplings among normal modes may set in
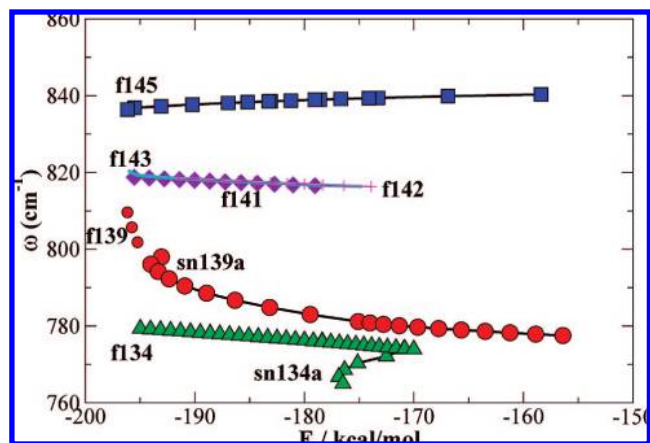

Figure 3. Continuation/bifurcation diagram of the active site of C*c*O, which depicts the evolution of the frequencies in a few families of periodic orbits with increasing the total energy. These families are mainly associated with the Fe=O bond oscillations. sn denotes saddle-node bifurcations.

even for very small excitation energies. Thus, it is necessary to find proper classical stationary structures which approximate the quantum mechanical eigenfunctions. Periodic orbits play such a role for the overtone states.[8] It has been proved that each normal mode is associated with at least one principal family of periodic orbits.[53] We call them families since they exist for a range of energies. We can plot the periods (T) or better the energy frequency ($\omega = 2\pi\hbar/T$) with respect to the total energy (E) of the molecule producing a projection of what is called continuation/bifurcation diagram.[54] Semiclassically, these frequencies approximate the energy differences of adjacent quantum energy levels.

In Figure 3 we plot such a diagram for those principal families that are mainly associated with the ferryl-oxo bond harmonic oscillations. The labels correspond to the harmonic normal modes from which the family originates. We can see three major frequency regions. The low-frequency f134 family corresponds to a breathing mode of the imidazole in the proximal area of iron. The f139 is associated with an oscillation of Fe−N bond, but it appears to be highly anharmonic. This anharmonicity results in a saddle-node bifurcation, sn139a. We have extensively discussed the appearance of the new POs from a saddle-node bifurcation, since they create islands of stability in chaotic regions of phase space.[55] Saddle-node bifurcations have been seen in most of triatomic molecules that we have studied, and recently in alanine dipeptide.[46] They create new type of motions which sometimes are highly localized in a bond.

The f139 family of POs is an example of how anharmonicity and coupling to other degrees of freedom can drastically change the harmonic vibrational frequency of the mode even with a small increase in energy. Unfortunately, it is difficult to foresee such nonlinear phenomena in advance. Usually, spectroscopic investigations or detailed calculations are required.

The middle frequency families, f141, f142 and f143 differ only by a few wavenumbers and show small anharmonicities. They involve oscillations of Fe with the porphyrin ring. The higher frequency periodic orbits of the f145 family show negative anharmonicity and represent asymmetric oscillations

(48) Pople, J. A.; Scott, A. P.; Wong, M. W.; Radom, L. J. *Isr. J. Chem.* **1993**, *33*, 345–350.
(49) Ghosh, A.; Skancke, A. *J. Phys. Chem. B* **1998**, *102*, 10087–10090.
(50) Pinakoulaki, E.; Pfitzner, U.; Ludwig, B.; Varotsis, C. *J. Biol. Chem.* **2003**, *278*, 18761–18766.
(51) Oda, K.; Ogura, T.; Appelman, E.; Yoshikawa, S. *FEBS Lett.* **2004**, *570*, 161–165.
(52) Rapaport, D. C. *The Art of Molecular Dynamics Simulation*; Cambridge University Press: London, 1995.

(53) Weinstein, A. *Inv. Math.* **1973**, *20*, 47–57.
(54) Farantos, S. C.; Qu, Z. W.; Zhu, H.; Schinke, R *Int. J. Bifurcations Chaos* **2006**, *16*, 1913–1928.
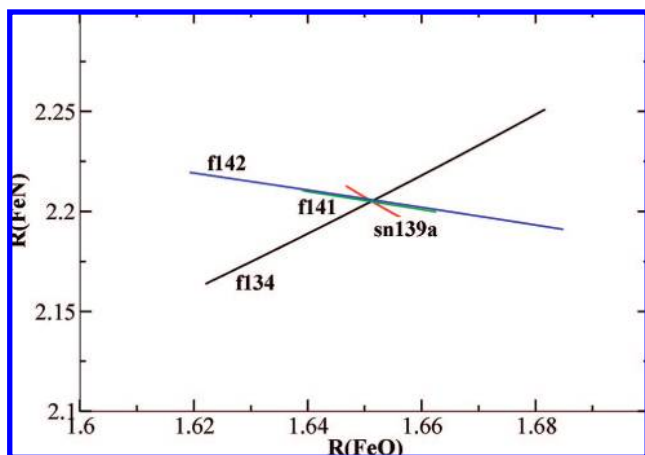(55) Farantos, S. C. *Int. Rev. Phys. Chem.* **1996**, *15*, 345–374.

Figure 4. Projections of representative periodic orbits on the plane of the two bonds (R_{FeO}, R_{FeN}). Distances are in angstroms and the energies of POs are approximately 3 kcal/mol above the minimum (−196.2 kcal/mol).

of the imidazole−Fe=O bonds. In all these families the hydroxyl group attached to Cu_B shows appreciable displacements.

POs, as closed threads in phase space, help to visualize the motions in the complex multidimensional coordinate space. Projections of the periodic orbits in the plane of the two bonds of iron in the distal and proximal region (R_{FeO}, R_{FeN}) for representative periodic orbits are shown in Figure 4. Their energies are about 3 kcal/mol above the minimum of the potential (−196.2 kcal/mol). For the f134 family the motions of the two bonds are in phase, whereas for the others the bonds oscillate in opposite phases. It is worth emphasizing that we have not found clearly localized motions on a single bond like Fe=O. Normal mode type motions prevail in the active site, at least for low excitation energies.

Examining the stability of periodic orbits, we found that most of them remain stable for all energies studied, except the f139 family which turns to singly unstable; i.e., only one degree of freedom is unstable. This means that the nearby trajectories can escape through the unstable degree of freedom, and thus explore larger regions of phase space. Stable periodic orbits trap the nearby trajectories for considerably longer times, and thus they contribute to coherent motions in the molecule.

To see how these periodic orbits affect the spectra, we integrate trajectories by randomly selecting the velocities of atoms and scaling them accordingly to achieve an average temperature of 300 K. From a time series of 2.5 ns for Fe=O bond, we produce the power spectrum shown in Figure 5a (i, ii, and iii). For comparison we depict several curves: the absolute Fe−^{16}O spectra of the active site without constraints (i) (blue curve), keeping the Fe−imidazole distance constant at its optimized value (ii) (red), and the Fe−N absolute spectrum of the active site when Fe−^{16}O distance is kept constant at its optimized value (iii) (dark yellow). In addition, the absolute Fe−^{16}O spectra including the effect of the protein matrix are shown in protonation case D (see text for propionate−Asp399 interaction in the next section) and Glu278 deprotonated with Fe−His411 distance constant at its optimized value (iv) (green), as well as Glu278 protonated without constraints (v) (gray curve).

In Figure 5a we can see that, by constraining the Fe−N (His411) bond to its crystallographic value, the 773 cm^{-1} band disappears (ii, red curve), while constraining the Fe=O distance the band with a peak at 776 cm^{-1} is the dominant
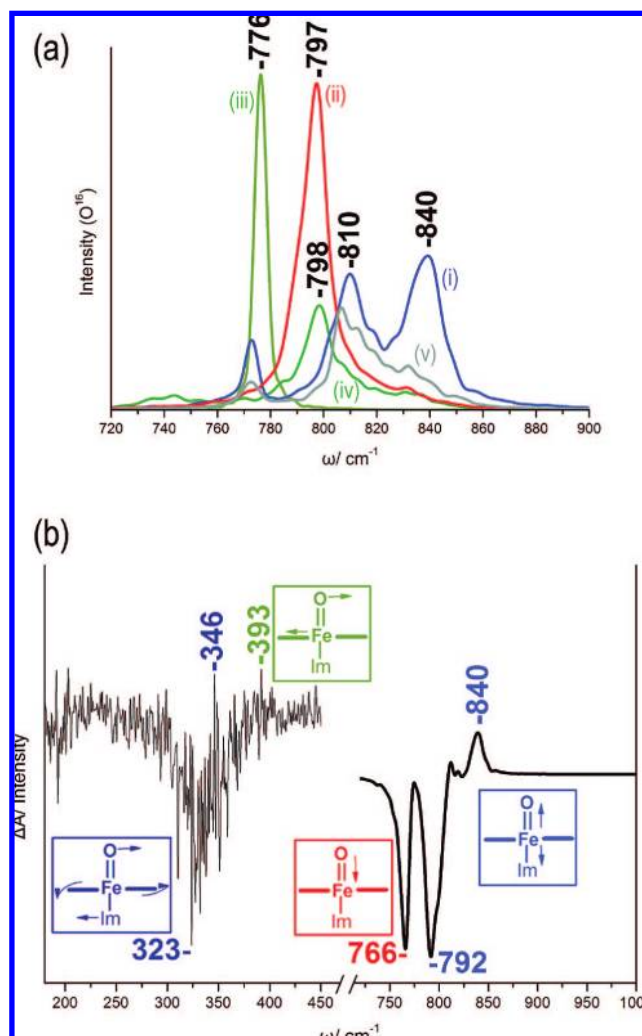

Figure 5. (a) Absolute (Fe−^{16}O) spectra of the active site (i) without constraints (blue curve) and (ii) with Fe−imidazole distance constant at its optimized value (red). (iii) (Fe−(N)imidazole) absolute spectrum of the active site when Fe−^{16}O distance is kept constant at its optimized value (dark yellow). In addition, absolute (Fe−^{16}O) spectra including the effect of the protein matrix are shown in protonation case D (see text for propionate−Asp399 interaction), where (iv) Glu278 is deprotonated with Fe−His411 distance constant at its optimized value (green) and (v) Glu278 protonated without constraints (gray). (b) Calculated difference spectrum (^{16}O minus ^{18}O), exhibiting features of Fe−O stretching (750−900 cm^{-1} region) and bending (300−400 cm^{-1} region) for the active site model. Graphical representation of selected modes corresponding to peaks in the spectrum are shown.

one in the ν(FeN) spectrum for the same spectral region (700−860 cm^{-1}) (iii, dark yellow). In accordance with the periodic orbit analysis, we assign the 773 cm^{-1} peak to a breathing motion of imidazole at the proximal region of iron. Comparing spectra of the total protein to those of the active site (curves i and v), we can immediately deduce that the spectroscopic features of Fe=O stretch remain. The good agreement in the positions of the peaks at 798 cm^{-1} demonstrates that the active site alone can reproduce vibrational frequencies of the enzyme.

In Figure 5b the calculated difference spectrum (^{16}O minus ^{18}O), exhibiting features of Fe−O stretching (750−900 cm^{-1} region) and bending (300−400 cm^{-1} region) for the active site model are shown. The latter appears with considerably lower intensity, and thus we give these differences without smoothing the spectrum but with significant magnification
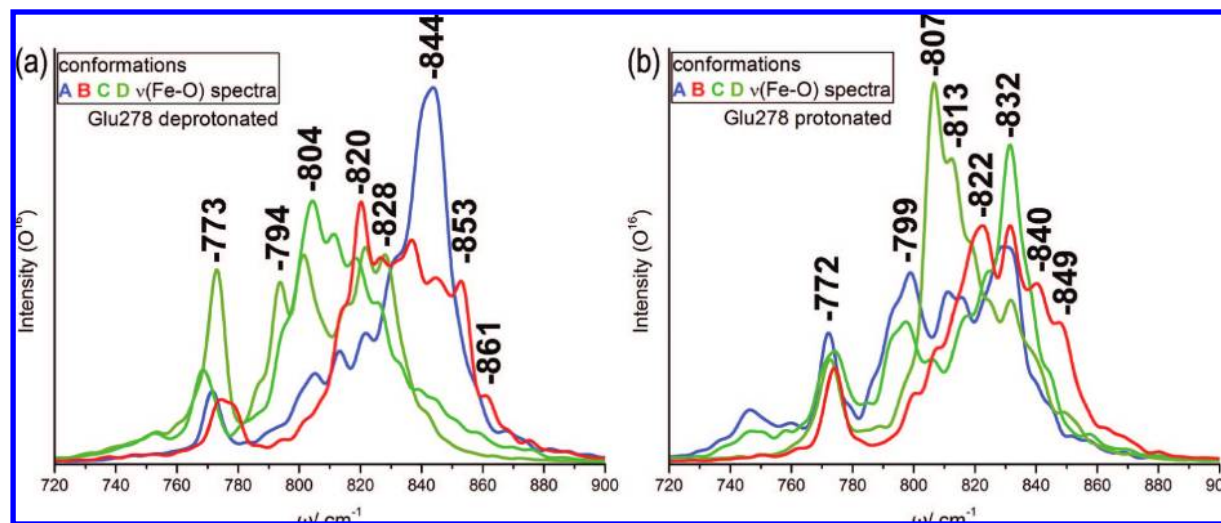
Figure 6. Calculated Fe=O power spectra of A, B, C, and D protonated/deprotonated states of the enzyme (see text) when Glu278 is deprotonated (a) or protonated (b). Simulations were carried out at 300 K.

of the intensities. We have decided not to pursue further the study of these vibrational modes in the present work. Finally, it is worth noticing in Figure 5b the two negative peaks in the 750−900 cm^{-1} region which also appear in the difference spectrum of the DFT calculations (Figure 2b).

The smoothed absolute spectrum of the active site (i, blue curve) exhibits three bands, 773, 810−820, and 840 cm^{-1}, in accordance to the POs analysis. How are these bands affected by the protein environment and how do they change in the protonated/deprotonated counterparts? In the next section we investigate these questions.

C. Spectra of C*c*O and Its Protonated States. Molecular dynamics simulations at 300 K were carried out with initial Cartesian coordinates taken from the two-subunit of *aa₃* crystal structure of *Paracoccus denitrificans* which has a size of approximately 12 000 atoms in total. Protonated/deprotonated structures resulting from the interaction of the propionate of the heme *a₃* pyrrole ring A and amino acid Asp399 are used to examine the role of these events in the spectra of ferryl-oxo intermediates. The protonated/deprotonated A, B, C, and D conformations are described in Figure 1. In structures A and C all carboxyl groups in equilibrium are protonated or deprotonated, respectively, while in B or D structures only one H$^+$ is available protonating either Asp399 or propionate, respectively.

We integrate the classical equations of motion with constant energy for approximately 1.2 ns. After 100 ps equilibration we store time series of ferryl-oxo bond. The calculated power spectra are shown in Figure 6. The plot on the left corresponds to the deprotonated Glu278 case and that on the right to protonated Glu278. These rather congested graphs allow us to make two significant remarks. First, the well-separated band at about 773 cm^{-1} remains practically stable for all protonated/deprotonated states of C*c*O studied. Second, the rest of the spectrum covers the same frequency interval (780−860 cm^{-1}), approximately having peaks at the same frequencies (marked on the plot), although with variable intensities. These frequencies are in proximity to those found in the spectrum of the active site. An example was given in Figure 5a where the spectrum of the active site (i) and that of the D structure for the protonated Glu278 case (v) were compared. Although there are differences in the intensities

of the lines, we find only small displacements in their positions. These results support the conclusion about the localization of the motions in the active site, and thus, a good description of the spectra can be obtained by studying the more convenient smaller size chemical species.

In Figure 7 we depict the difference spectra obtained from ^{16}O minus ^{18}O isotopic substitution of Fe^{IV} and Cu$_B^{II}$ oxygens. The projection of all spectra in one plot allows us to draw conclusions for all protonated/deprotonated states simultaneously and to compare with the experimental results. For most of them, two bands can clearly be seen which cover a width of frequencies of approximately 50 cm^{-1}. This is in accordance with the experimental observations.[21−25] Although in these publications the dominant lines are discussed, they do show broad bands of about 50 cm^{-1} width. Furthermore, it is worth noticing the good agreement of the 807 cm^{-1} peak found for the D/Glu278 protonated structure with the experimentally reported value.

It is also interesting to note that the differences between the peaks of isotopomers are approximately 30−50 cm^{-1}; for example in the D/Glu278 protonated structure the pair of frequencies (832, 797 cm^{-1}) and (807, 770 cm^{-1}) are tabulated. We attribute the differences to more localized motions of the Fe^{IV}=O bond in the large system. It is expected that for a local bond mode the frequency shift to be given by the factor $\omega_{18}/\omega_{16} \approx (m_{16}/m_{18})^{1/2}$, where ($m_{16}$, m_{18}) denote the masses of two oxygen isotopes. In the bulk protein the iron is stabilized to one of the helices via His411 (see Figure 1), thus increasing its effective mass, whereas in the isolated active site the normal modes represent more collective type motions. Evidence for the influence of the proximal histidine on iron were given before. On constrained Fe−N cases (D structure (iv) and active site (ii) in Figure 5a), the proximal histidine influence is absent, leading to two almost identical spectra, irrelevant to the presence of protein matrix, while for the unconstrained cases (active site (i) in Figure 5a and A, B, C, and D structures in Figure 6) several differences emerge.

The calculations demonstrate that multiple peaks may appear in the vibrational spectra of cytochrome *c* oxidase as a result of the presence of different protonated structures but with the same oxidation state of the binuclear center. However, it is important to emphasize that the vibrational
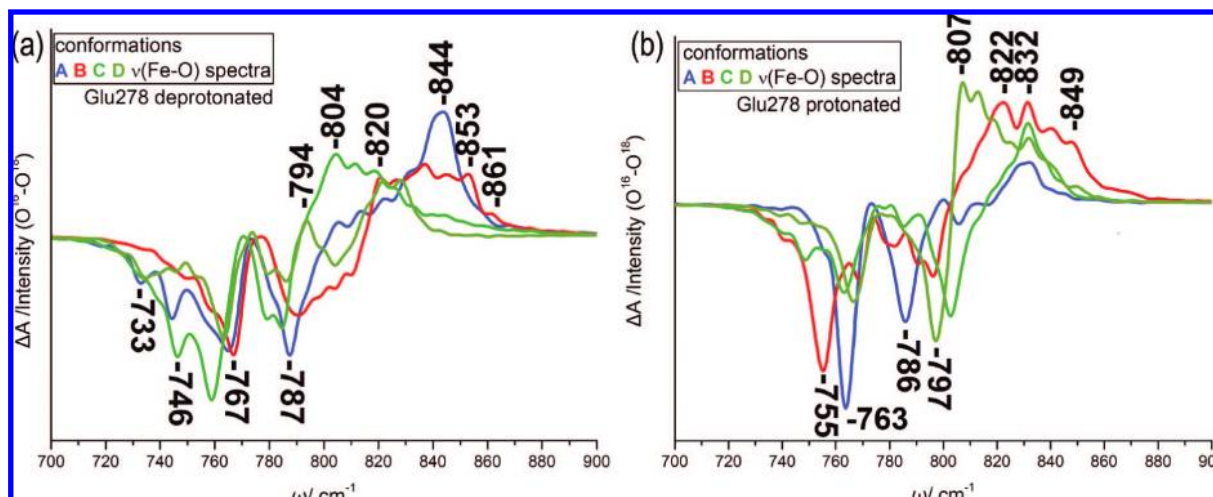
Figure 7. Difference spectra of isotopically substituted oxygen (^{16}O minus ^{18}O) for all protonated/deprotonated structures of CcO studied. Plots (a) for the deprotonated Glu278 and plots (b) for the protonated Glu278 amino acid.

mode frequencies are not altered significantly and only the intensities vary by changing the Coulombic environment of the active site. One could suggest that protonation events in the region of propionates would affect the electrostatic charge felt by the Fe^{IV}=O moiety altering its vibrational frequency. For this purpose, we have performed additional DFT calculations, but in lower level of theory (blyp/TZVP triple-ζ basis set) with the software package Turbomole.[56] In this case, Cu$_B$ site is absent in the models, while iron porphyrin contains only the ring A propionate side chain along with His403/ Asp399 (*P. denitrificans* numbering) residues in close contact. Three cases are studied; in the first, a proton is shared between propionate and Asp399, in the second, a proton is shared between propionate and His403, and in the last, no proton is present on the propionates/His403/Asp399 site. Calculated vibrational frequencies on the same level of theory (blyp/TZVP) exert a maximum ν(Fe−O) shift of 4 cm^{-1}, which is negligible. Contrary to that, the environment of proximal histidine (His411) consists of amino acids like Gly386 and Thr389, both hydrogen bonded to it (Figure 1), which could affect either its basicity or behavior in general.

IV. Conclusions

Spectroscopy requires reliable theoretical models to interpret spectral lines and bands, a particularly difficult task for large biological molecules. In this article, we have shown that with a systematic approach which employs methods of nonlinear mechanics, we can study the vibrational spectra such as those of CcO protein. The comprehensive study of the active site of 95 atoms has allowed us to carry out DFT electronic structure calculations and to build a reliable potential function. The location of the principal families of periodic orbits which describe the anharmonic and coupled normal modes of the ferryl-oxo species offers a more realistic approach to study vibrational motions than the harmonic approximation. Remarkably, we find these stationary classical mechanical objects to remain stable for a considerable energy range, a fact which reveals coherent local motions. For small molecules, we have shown the correspondence of the

principal families of periodic orbits to quantum mechanical overtone states and in some cases to experimental spectra.[2,4,8]

One major outcome of the present study is that the observed frequencies in the active site do not change significantly when the protein frame is taken into account. The protonation of Glu278, Asp399, and A-propionate seems not to influence significantly the location of the bands but only their intensities. Thus, protonated/deprotonated structures of CcO vary the importance of one band (higher intensities) and that results in the appearance of one or two prominent positive bands in the difference spectra of isotopically substituted species such as the ferryl-oxo intermediates.

It was proposed, recently, that transfer of a proton (H$^+$) from E278 (*P. denitrificans* numbering) to an unknown residue above hemes a/a_3 is the first step in the pumping mechanism by cytochrome c oxidase across the mitochondrial membrane.[57] During P → F transition, E278 is protonated via the D-pathway, its proton is then transferred to the active site and E278 is reprotonated, while a proton is released to the P-side.[57] The 804 and the 790 cm^{-1} peaks have previously been attributed to ferryl-oxo species at the P$_R$ and F level.[23−25] In addition, based on the oxidized-CcO/H$_2$O$_2$ reaction, the P (607 nm) intermediate generates the 804 cm^{-1} species, while the F (580 nm) intermediate, the 790 cm^{-1} species.[22,50]

A, B, C, and D conformations only differ in the protonation state, but not in their oxidation level. Thus, our molecular dynamics results consist a theoretical evidence that on the same oxidation level with oxo-ferryl character (based on the mixed valence form, Cu$_A^{1.5+}$−Cu$_A^{1.5+}$, heme a^{3+}, heme a_3^{2+}−Cu$_B^{1+}$) enhancement of low and/or higher frequencies, attributed to Fe^{IV}=O stretching mode, can occur in a vibrational spectrum depending on the protonation state of key intermediates around the active site. This is significant, as the 804/790 cm^{-1} prominent peaks have previously been attributed to two different oxidation states. Since protonation events occur during the P → F transition, we consider these experimentally observed vibrational modes to be, in fact, due to protein matrix conformational changes near the active site. In the case of D structure, where Fe−His411 distance is kept

(56) Ahlrichs, R.; Bär, M.; Häser, M.; Horn, H.; Kölmel, C. *Chem. Phys. Lett.* **1989**, *162*, 165−169.

(57) Bellevich, I.; Verkhovsky, M. I.; Wikstrom, M. K. *Nature* **2006**, *440*, 829−832.

constant, the spectrum matches that of the active site (Figure 5a (ii, iv)). This in fact orients our interest to the proximal site (His411) being the main contributor to the enhancement mechanism of different vibrations. In fact, conformational changes in the region of the ring A propionate of heme a_3, due to protonation events, are communicated via Asp399/His403 to Gly386/Thr389 in the proximal area altering H-bonding networks in the region, and thus controlling the effect of His411 on the Fe−O frequency. In such way we link significant intermediates of the proton pump mechanism to spectroscopic characteristics.

JA801840Y